

## Antenna Pattern of the Quasi-Optical Hot-Electron Bolometric Mixer at THz Frequencies

H.-W. Hübers<sup>a)1</sup>, A. D. Semenov<sup>a)</sup>, H. Richter<sup>a)</sup>, J. Schubert<sup>a)2</sup>, S. Hadjiloucas<sup>b)</sup>,  
J. W. Bowen<sup>b)</sup>, G.N. Gol'tsman<sup>c)</sup>, B.M. Voronov<sup>c)</sup>, and E.M. Gershenson<sup>c)</sup>

a) DLR Institute of Space Sensor Technology and Planetary Exploration,  
12489 Berlin, Germany

b) Department of Cybernetics, The University of Reading, Whiteknights,  
Reading RG6 6AY, United Kingdom

c) Physical Department, State Pedagogical University of Moscow,  
119891 Moscow, Russia

### Abstract

An investigation of the antenna pattern of a quasi-optical hot-electron bolometric mixer at terahertz (THz) frequencies is presented. The antenna consists of a logarithmic-spiral planar feed antenna which was mounted on the back side of a hemispherical lens with an extension length optimized for 2.5 THz. The power patterns were measured at several frequencies between 0.7 THz and 4.3 THz for two orthogonal polarizations. The level of the first sidelobe is smallest at 2.5 THz. The sidelobes are different for both polarizations and the main lobes are wider than predicted by diffraction at the diameter of the lens. This indicates that the pattern is not only determined by the lens but also by the feed antenna. The antenna pattern measured by heterodyne detection has almost the same width as the power pattern but significantly higher sidelobes. At 1.6 THz the phase pattern of the hybrid antenna was measured with a quasi-optical interferometric technique.

### 1. Introduction

The hot-electron bolometer (HEB) is the mixer of choice for heterodyne receivers at terahertz (THz) frequencies, where SIS mixers and Schottky mixers are not sensitive enough for ultimate, quantum limited performance. It has been shown that quasi-optically coupled HEB mixers have noise temperatures close to the quantum limit [1,2,3,4], an intermediate frequency bandwidth up to 9 GHz [3,4,5,6], and require local oscillator power less than 1  $\mu$ W [1,2,3,4].

At this quite advanced stage of HEB mixer development it becomes increasingly important to characterize precisely the antenna pattern of the quasi-optical HEB mixer at

---

<sup>1</sup> heinz-wilhelm.huebers@dlr.de

<sup>2</sup> Present address: Max-Planck Institut für Extraterrestrische Physik, 85740 Garching, Germany

THz frequencies. The knowledge of the antenna pattern is of prime importance for any practical application since it allows to achieve optimal coupling of the receiver to a telescope as well as accurate retrieval of atmospheric data. At frequencies below about 1 THz waveguide coupled mixers are commonly used. The performance of waveguide antennas is excellent at these frequencies. However, beyond 1 THz losses of the waveguide increase. Additionally, fabrication becomes more difficult and costly. An alternative approach is the combination of a planar antenna with a lens. In this quasi-optical design the mixer and a planar antenna are fabricated on a substrate which is mounted on the back side of a lens. The lens is made from the same material or a material with similar refractive index as the substrate. Different types of lenses and planar antennas have been investigated [7,8]. Depending on the actual requirements such as Gaussian coupling efficiency and directivity either extended hemispherical lenses or elliptical lenses are used. If the feed antenna is placed in the aplanatic focus of a hemispherical lens it is called hyperhemispherical lens. At a certain extension length the antenna pattern is determined by the diffraction limit of the lens. If the planar feed antenna is placed at this position it is called hybrid antenna [7]. In fact the hybrid antenna is a good approximation to the elliptical lens-antenna. The hyperhemispherical antenna yields a better Gaussian coupling efficiency than the hybrid antenna or the elliptical lens-antenna but the directivity is worse [8]. In this paper we investigate the antenna performance of a HEB mixer integrated in a hybrid antenna with a logarithmic-spiral feed.

## 2. Antenna Design

The investigated HEB mixers were made from a 3.5 nm thick superconducting NbN film. The film was deposited by dc reactive magnetron sputtering onto a 350  $\mu\text{m}$  thick high resistivity Si substrate (5  $\text{k}\Omega\text{cm}$ ). The bolometer itself is a 1.4  $\mu\text{m}$  wide and 0.2  $\mu\text{m}$  long bridge. It has a transition temperature of about 9 K. The HEB is located in the center of a planar two-arm logarithmic-spiral antenna, which couples both the signal and the local oscillator (LO) radiation with the bolometer (Fig. 1). The central part of the antenna was patterned using electron beam lithography while the outer part was defined by conventional UV photolithography. The diameter of the circle that circumscribes the spiral structure is 130  $\mu\text{m}$ . This effectively determines the longest wavelength above which the properties of the feed antenna are no longer independent of the wavelength. The wavelength inside the silicon should be less than twice the diameter of this circle. In our case this yields a long wavelength limit outside the silicon of 884  $\mu\text{m}$  (0.34 THz). The shortest wavelength should be at least 10 times larger than the radius of the inner circle, inside which the antenna arms form inner terminals and deviate from the ideal spiral shape. The inner circle has a diameter of about 2.2  $\mu\text{m}$  yielding a short wavelength cut-off of 37  $\mu\text{m}$  (8 THz). However it should be pointed out that the wavelength limits are an estimate and have to be verified experimentally. Between the circles, the antenna arms make two full turns. A radial line from the origin of the antenna intersects a spiral arm at an angle of 70°.

The substrate supporting the HEB with the planar antenna was glued onto the flat side of an extended hemispherical lens. The lenses are spheres with either 6 mm or 12 mm diameter, which were cut off from optically polished, high resistivity ( $>10 \text{ k}\Omega \text{ cm}$ ) silicon. Lenses with and without an antireflection coating from Parylene C were investigated [9]. The extension of the lens together with the substrate yields a total extension length of 1.2 mm and 2.4 mm for the 6 mm lens and for the 12 mm lens, respectively. This is the optimal extension length, for which the beam pattern of the hybrid antenna is predicted to be diffraction limited, i.e. the pattern is rather determined by the diameter of the lens than by the beam properties of the planar feed antenna. It is worth mentioning that in the range of the diameter to wavelength ratios, which we covered in the experiments, the optimal extension length weakly depends on the wavelength [7].

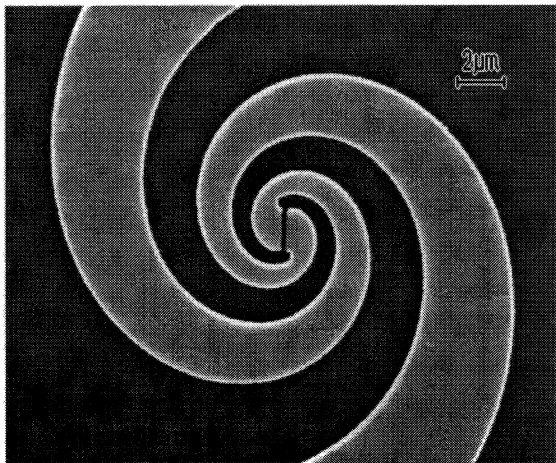


Fig. 1: Layout of the logarithmic-spiral antenna. The HEB is located in the gap in the center of the spiral arms. It is  $0.2 \mu\text{m}$  long and  $1.4 \mu\text{m}$  wide. The inner circle where the spiral deviates from the ideal shape has a diameter of  $2.2 \mu\text{m}$ .

### 3. Antenna Power Pattern

The power patterns of different hybrid antennas have been measured 0.7 THz, 1.4 THz, 1.6 THz, 2.5 THz, 3.1 THz and 4.3 THz. The temperature of the HEB was set slightly below the transition temperature of the superconducting bridge and the HEB was biased with constant current. The dewar with the HEB was placed on a rotation table in the far field ( $3\text{-}10 \times$  Rayleigh distance) of an optically pumped far-infrared gas laser. The HEB was located in the center of rotation. The laser radiation was chopped and the signal delivered by the HEB was measured as a function of the angle of rotation. Patterns were measured by rotating the HEB around the axis parallel to its length. The polarization of the incoming radiation was determined by a wire grid. For E-plane measurements the vector of the electric field of the laser radiation is parallel to the width of the superconducting bridge while for H-plane measurements it is parallel to the length. Some examples of the power patterns are shown in Fig. 2.

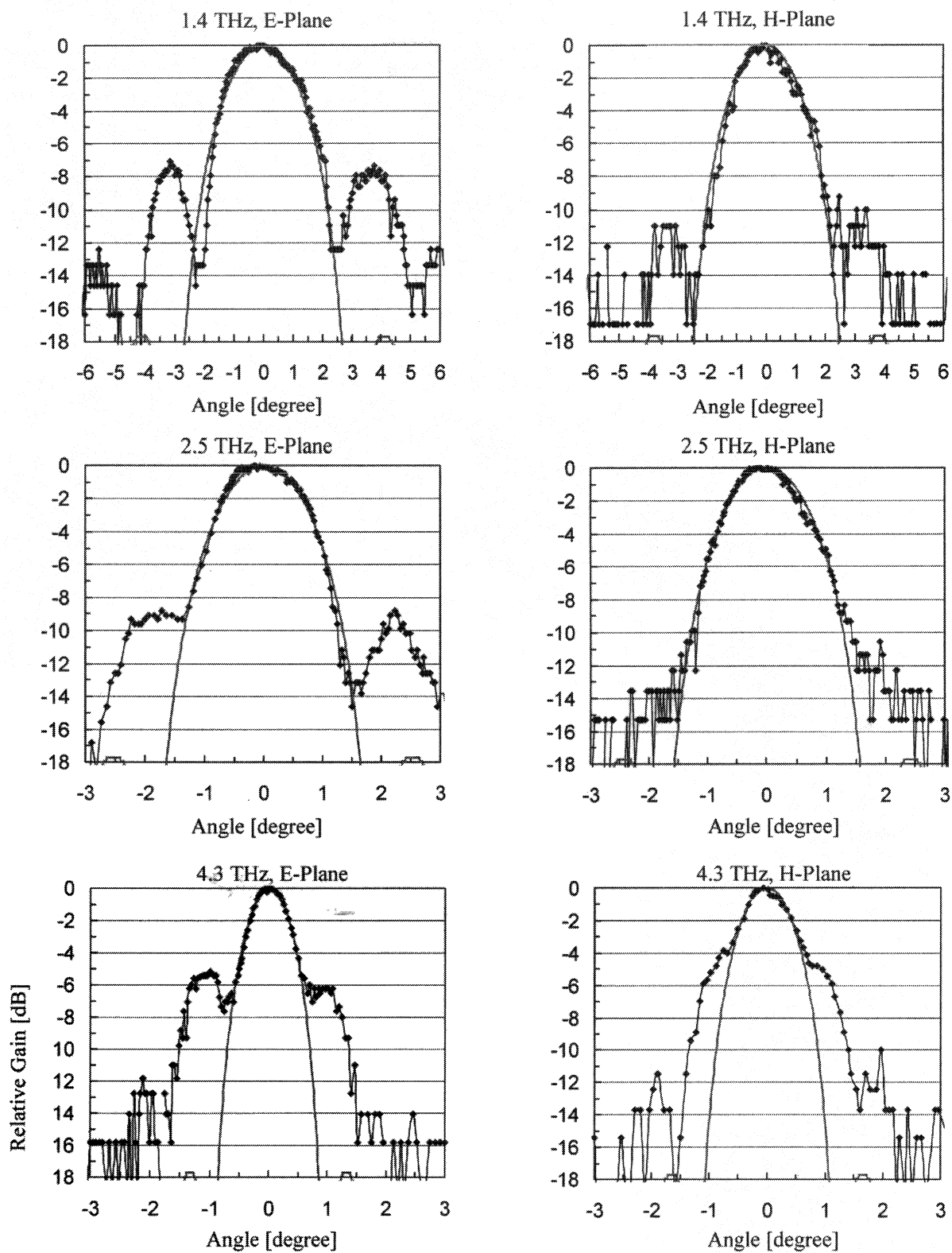


Fig. 2: Antenna power patterns at different frequencies and in two orthogonal polarizations (E- and H- plane refer to polarization of the laser radiation, see text).

The solid lines represent the diffraction limited antenna patterns that were simulated according to the expression  $(2J_1(\nu)/\nu)^2$ , where  $\nu = (\pi \tan(\theta) d)/\lambda$ ,  $J_1$  is the Bessel function of the first kind,  $\theta$  is the angle of rotation and  $d$  is an effective diffracting aperture, which was varied to yield the best fit to the main lobe of the measured pattern. In Fig. 3 the results are summarized. The first sidelobe is lowest at 118.8  $\mu\text{m}$  (2.5 THz) which is the wavelength for which the extension length of the hybrid antenna is optimal. Towards longer wavelengths the level of the first sidelobe increases slightly because the extension length is longer than the optimum one. At the two shortest wavelengths the first sidelobes are highest. This might be attributed to contributions from the inner part of the feed antenna where the spiral deviates from the ideal shape. In general the sidelobes are higher than predicted by simple diffraction theory of a uniform wave at a circular aperture. This is partly due to internal reflections. Additionally, the sidelobes in the E-plane are always higher than in the H-plane except for the two shortest wavelengths. These findings indicate that the pattern of the log-spiral feed antenna is not rotational symmetric and does not illuminate the diameter of the lens uniformly.

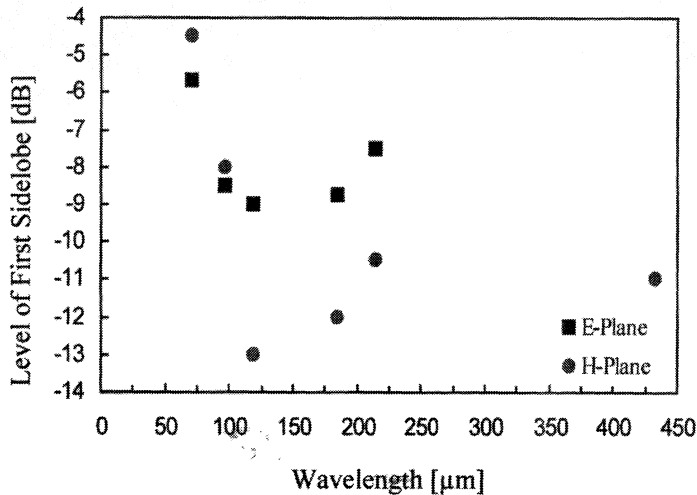


Fig. 3: Level of the first sidelobe as a function of wavelength for E- and H-plane.

Fig. 4 displays the FWHM as a function of the wavelength for E- and H-plane patterns. The dashed line is a linear fit to the data while the solid line represents the FWHM as expected for an antenna pattern which is diffraction limited by the diameter of the lens. The optimum extension length of a hybrid antenna made from silicon is almost constant in the wavelength range considered here. Therefore the linear dependence of the FWHM on the wavelength indicates that diffraction dominates the width of the antenna pattern. The difference between measurement and prediction might be explained by a non-uniform illumination of the lens by the feed antenna. Because of the high refractive index of silicon compared to quartz, this effect is more pronounced in a hybrid antenna made from silicon than in one made from quartz. The optimum extension length at given wavelength and diameter of the lens is smaller in silicon than in quartz. This results in a lower edge taper for a silicon hybrid antenna than for a quartz hybrid antenna. This in turn yields a smaller FWHM for the silicon hybrid antenna. For a quartz hybrid antenna the FWHM is larger and agrees better with the width determined by diffraction the lens diameter.

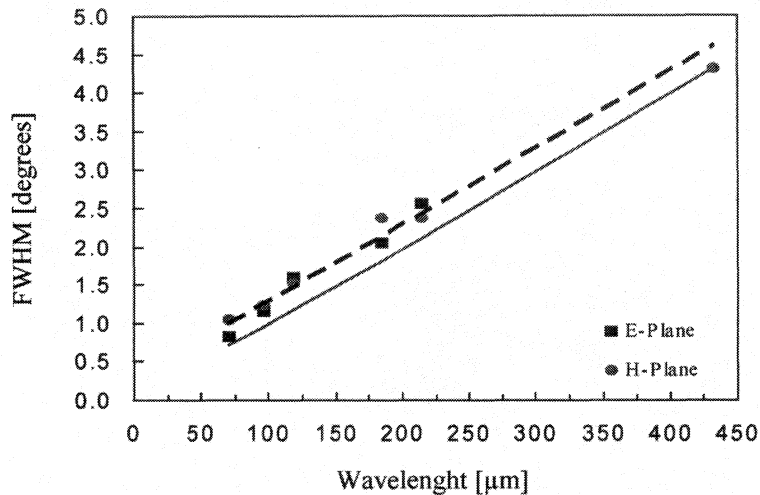


Fig. 4: FWHM as a function of the wavelength. The solid line represents the diffraction limit as given by the diameter of the lens while the dashed line is a linear fit to the measured FWHM.

#### 4. Heterodyne Antenna Pattern

For designing a practical heterodyne receiver the antenna pattern measured in the heterodyne mode is the relevant one. This pattern may differ from the antenna power pattern since heterodyne detection preserves the phase information. We have performed measurements of the antenna pattern in the heterodyne mode. The hybrid antenna consisted of a 12 mm diameter silicon lens with a Parylene anti-reflection coating and a log-spiral feed antenna as described above. Again, the extension length was optimized for 2.5 THz. In principle, a standard Y-factor measurement setup as described previously [1] is used. However, instead of a liquid nitrogen cold load a small ( $0.14^\circ$  angular width) metal halide hot source is used. It can be moved in a plane orthogonal to the axis defined by the center of the main lobe of the antenna. The double sideband (DSB) signal is measured as a function of the position of the hot source. The heterodyne antenna pattern is given by the DSB signal as a function of the angle under which the hot source is seen by the HEB mixer. Fig. 5 displays the antenna patterns measured at 0.7 THz, 1.6 THz and 2.5 THz. The polarization of the FIR laser local oscillator is arbitrary since a rotatable wire grid is used to adjust the power from the FIR gas laser to the level which yields the best signal to noise ratio. At all frequencies the first sidelobe is significantly higher in the heterodyne pattern than in the power pattern and it increases with frequency. The FWHM is almost the same in the heterodyne and power patterns except at 2.5 THz where it is bigger in the heterodyne pattern. This is possibly due to a contribution from the high sidelobe to the main lobe. The reason for the high sidelobes is not clear yet. One possible explanation could be a strong change of the phase across the main lobe of the power pattern as it will be discussed in the next section. However, the power patterns were measured with an uncoated 6 mm lens while the heterodyne patterns were measured with a 12 mm anti-reflection coated lens. We would like to emphasize here that the spectral properties of our antenna are effected not only by the smaller radius of the spiral but also by the actual size of the HEB. This seems to be a general feature of planar antennas, since it was also noticed for twin-slot antennas [10]. For our log-spiral

antenna we found that, according to simulations [1], decrease of the HEB width flattens the frequency dependence of the noise temperature. The difference in the DSB noise temperature between 0.6 THz and 2.5 THz was reduced from 2.8 dB for a 1.7  $\mu\text{m}$  wide HEB to 1.5 dB for a 1.4  $\mu\text{m}$  wide HEB. Here again, the 1.7  $\mu\text{m}$  HEB was mounted on the uncoated 6 mm lens while the 1.4  $\mu\text{m}$  HEB was mounted on the 12 mm coated lens. All this makes comparison and interpretation of antenna patterns at different frequencies more difficult.

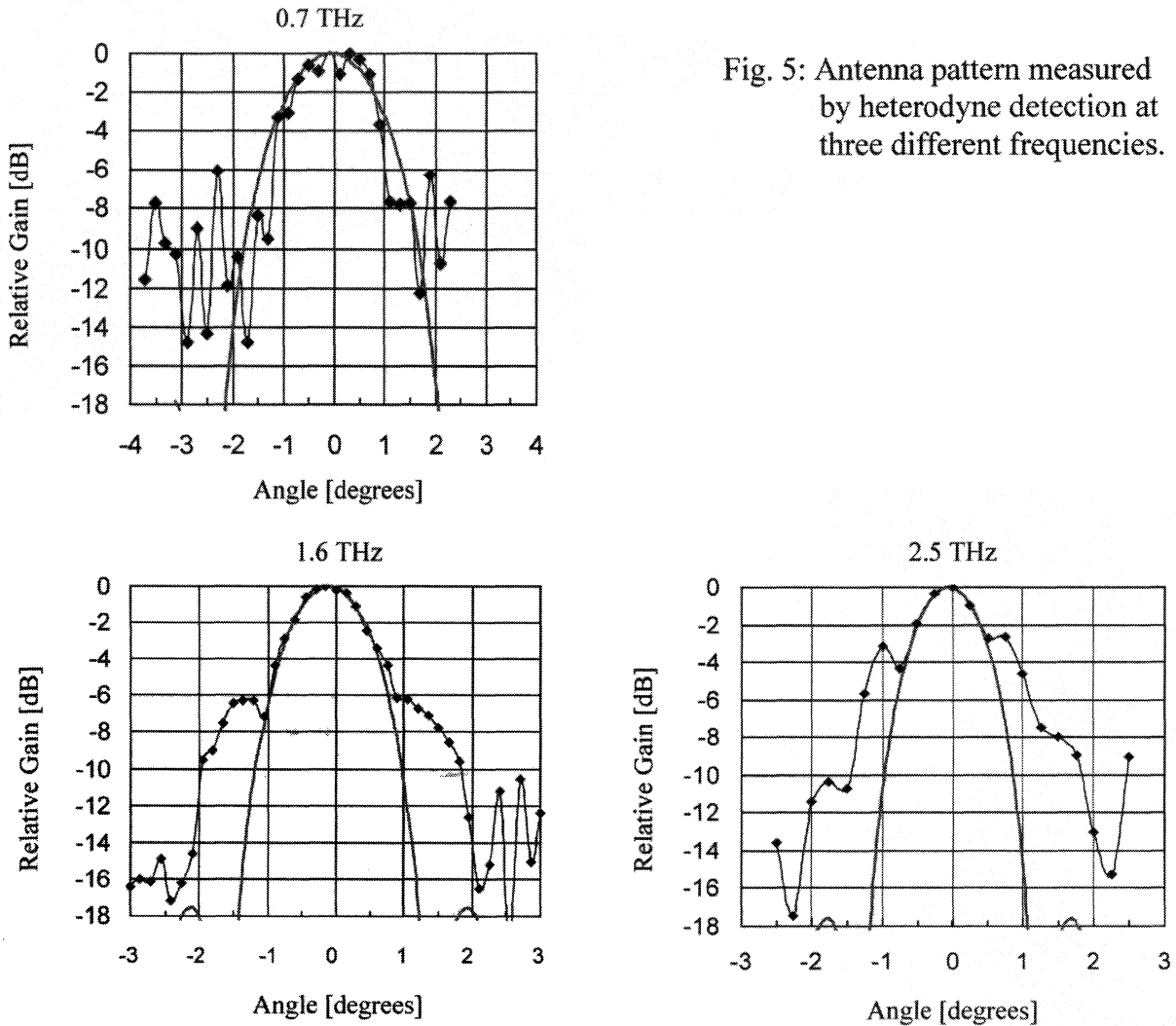


Fig. 5: Antenna pattern measured by heterodyne detection at three different frequencies.

### 5. Phase Measurements

Phase pattern measurements at frequencies towards or above 1 THz become increasingly problematic because it is difficult to provide a coherent phase reference. In our measurements we use a novel, quasi-optical interferometric technique to record both amplitude and phase pattern of antenna [11]. This method has been verified with a

Schottky mixer in a corner cube mount at 1.4 THz [12]. The principle is depicted in Fig. 6. The output radiation from a FIR gas laser is split by a 45° wire grid. A vertical wire grid is used in transmission and a horizontal wire grid is used in reflection. This set-up results in two mutually coherent co-polar sources S<sub>1</sub> and S<sub>2</sub>, each launching a beam towards a test antenna at slightly different angles θ and θ+θ<sub>s</sub>, where θ<sub>s</sub> is the angle subtended by the two sources. The two beams have a phase delay φ<sub>d</sub>. By blocking first one source and then the other, the power patterns V<sub>1</sub> and V<sub>2</sub> are measured as a function of the angle θ. Finally, the power pattern V<sub>12</sub> is measured when both sources launch a beam towards the HEB. The phase relation is extracted from the three power patterns according to

$$\Phi(\theta + \theta_s) - \Phi(\theta) + \Phi_d = \cos^{-1} \left\{ \frac{V_{12}(\theta) - V_1(\theta) - V_2(\theta)}{2\sqrt{V_1(\theta) \cdot V_2(\theta)}} \right\} \quad (1)$$

Since Φ<sub>d</sub> is independent of θ and the phase reference it can be set to zero. If V<sub>12</sub>(θ), V<sub>1</sub>(θ), and V<sub>2</sub>(θ) are measured the relative phase between successive directions which are separated by θ<sub>s</sub> can be determined.

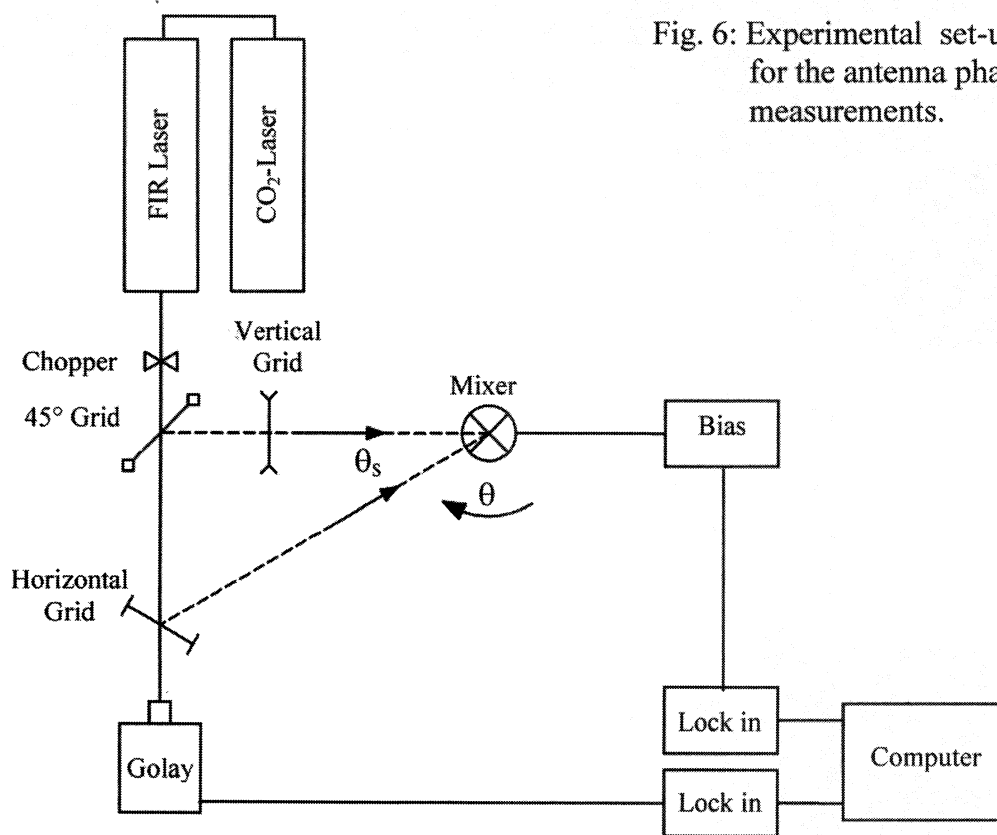


Fig. 6: Experimental set-up for the antenna phase measurements.

In Fig. 7 power and phase patterns measured at a frequency of 1.6 THz in the E-plane of the FIR laser are shown. The hybrid antenna consisted of a 6 mm lens without anti-reflection coating and the above described log-spiral feed antenna. FWHM and the level of the first sidelobe agree with the power patterns presented in section 3. The minimum phase difference occurs at a different position than the maximum of the main lobe. Also, there is no flat part of the phase inside the main lobe of the power pattern. This indicates that the HEB was not exactly positioned at the phase center. This position has to be determined by finding the pivot position that gives maximum phase flatness over the main lobe. However, the phase pattern of the hybrid antenna has changes quite drastically by about 0.3 –1.2 rad/degree. In contrast, the  $4\lambda$  quasi-optical Schottky mixer at 1.4 THz has a flat phase within the -6 dB points of the main lobe and the change of the phase outside the main lobe of the power pattern is  $< 0.2$  rad/degree. This indicates that the strong change of the phase of the hybrid antenna may contribute to the high level of sidelobes seen in the heterodyne antenna pattern. However, further investigations are necessary.

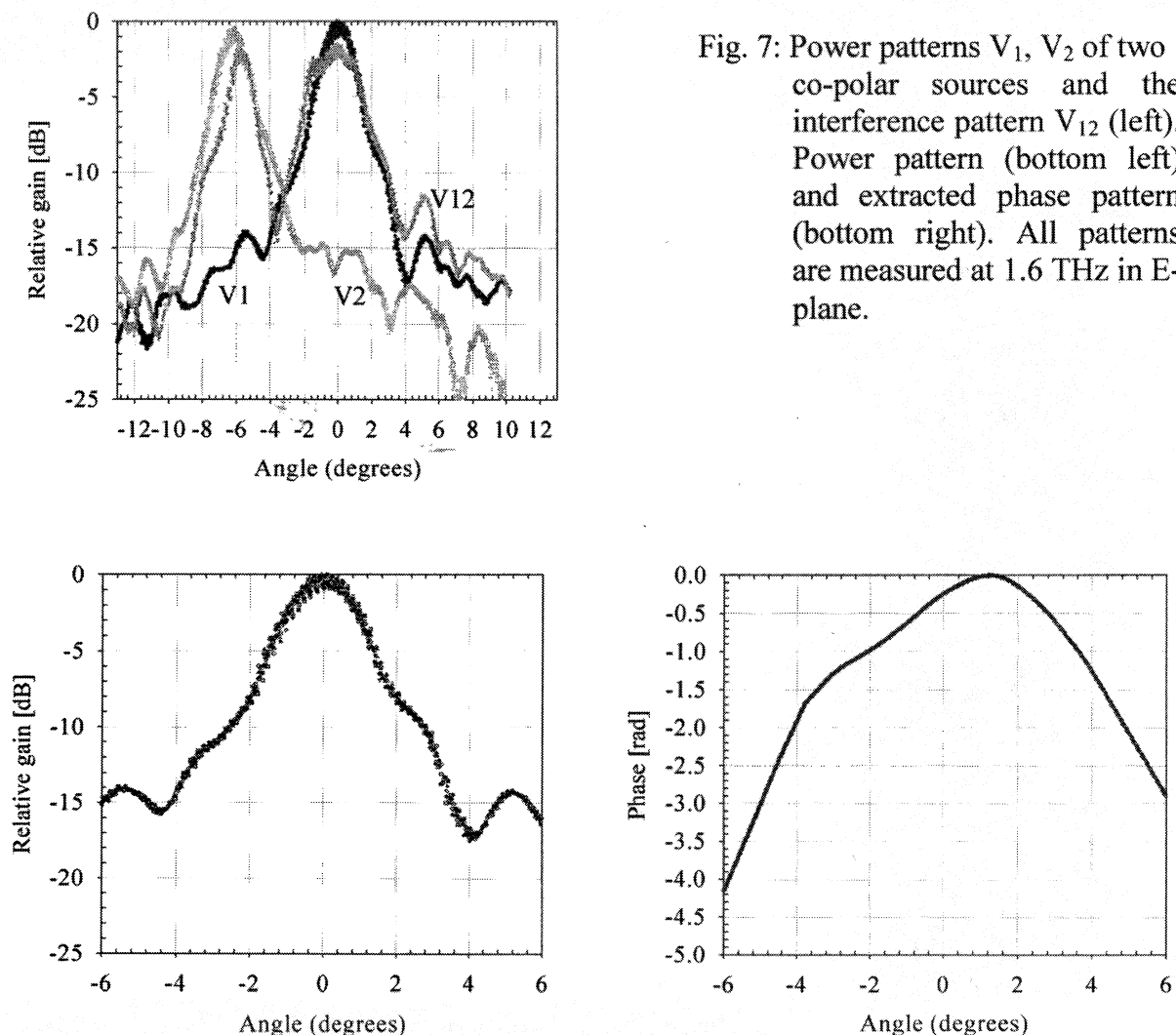


Fig. 7: Power patterns  $V_1$ ,  $V_2$  of two co-polar sources and the interference pattern  $V_{12}$  (left). Power pattern (bottom left) and extracted phase pattern (bottom right). All patterns are measured at 1.6 THz in E-plane.

## 6. Summary and Conclusions

We have investigated the beam pattern of a HEB mixer with a hybrid antenna. The antenna consists of a log-spiral feed antenna and a silicon lens. The power pattern was measured in the frequency range from 0.7 THz to 4.3 THz. It was found that the FWHM of the main lobe is wider and the sidelobes are higher than predicted by diffraction of a uniform wave at the aperture given by the diameter of the silicon lens. This can be attributed to a non-uniform illumination of the lens by the feed antenna. Measurements of the antenna pattern by heterodyne detection at 0.7 THz, 1.6 THz and 2.5 THz reveal that the sidelobes are higher than in the power patterns while the FWHM is almost the same. The phase of the hybrid antenna has been determined by a quasi-optical interferometric method. It is not constant across the main lobe of the power pattern. The results emphasize the importance of heterodyne antenna measurements and phase measurements. However, further investigations are necessary in order to get a complete understanding of the antenna pattern of a hybrid antenna at THz frequencies.

## Acknowledgement

This work was financially supported by the German Ministry of Science and Education (WTZ RUS-149-97), the European TMR project "INTERACT", NATO Division of Scientific Affairs, and the INTAS grant 99-0569.

## References

- [1] A. D. Semenov, H.-W. Hübers, J. Schubert, G. N. Golt'sman, A. I. Elantiev, B. M. Voronov, and E. M. Gershenson, "Design and performance of the lattice-cooled hot-electron terahertz mixer", *J. Appl. Phys.* **88**, 6758 (2000).
- [2] E. Gerecht, C. F. Musante, Y. Zhuang, M. Ji, K. S. Yngvesson, T. Goyette, and J. Waldman, "Development of focal plane arrays utilizing NbN hot electron bolometric mixers for the THz region", *Proc. of the 11<sup>th</sup> Int. Symp. on Space Terahertz Technol.*, 209 (2000).
- [3] M. Kroug, S. Cherednichenko, H. Merkel, E. Kollberg, B. Voronov, G. Gol'tsman, H.-W. Hübers, and H. Richter, "NbN HEB mixer for terahertz heterodyne receivers" *Proc. of the Int. Conf. on Appl. Superconductivity, Virginia Beach* (2000).
- [4] R. Wyss, B. Karasik, W. McGrath, B. Bumble, and H. LeDuc, "Noise and bandwidth measurements of diffusion cooled Nb hot-electron bolometer mixers at frequencies above the superconductive energy gap", *Proc. of the 10<sup>th</sup> Int. Symp. on Space Terahertz Technol.*, 214 (1999).
- [5] S. Cherednichenko, M. Kroug, P. Yagoubov, H. Merkel, E. Kollberg, K. S. Yngvesson, B. Voronov, and G. Gol'tsman, "IF bandwidth of phonon cooled HEB mixers made from NbN films on MgO substrates", *Proc. of the 11<sup>th</sup> Int. Symp. on Space Terahertz Technol.*, 219 (2000).

- [6] A. D. Semenov, H.-W. Hübers, "Frequency Bandwidth of a Hot-Electron Mixer According to the Hot-Spot Model", Proc. of the Int. Conf. on Appl. Superconductivity, Virginia Beach (2000).
- [7] T. H. Büttgenbach, "An improved solution for integrated array optics in quasi-optical mm and submm receivers: the hybrid antenna", IEEE Trans. Microwave Theory Tech. **41**, 1750 (1993).
- [8] D. F. Filipovic, S. S. Gearhart, and G. M. Rebeiz, "Double-slot antennas on extended hemispherical and elliptical silicon dielectric lenses", IEEE Trans. Microwave Theory Tech. **41**, 1738 (1993).
- [9] H.-W. Hübers, J. Schubert, A. Krabbe, M. Birk, G. Wagner, A. Semenov, G. Gol'tsman, B. Voronov, and E. Gershenzon, "Parylene anti-reflection coating of a quasi-optical hot-electron bolometric mixer at terahertz frequencies", Infrared Phys. and Technol. **42**, 41 (2000).
- [10] R. A. Wyss, A. Neto, W. R. McGrath, B. Bumble, H. LeDuc, "Submillimeter-wave spectral response of twin-slot antennas coupled to hot-electron bolometers", Proc. of the 11<sup>th</sup> Int. Symp. on Space Terahertz Technol., 388 (2000).
- [11] J. W. Bowen, S. Hadjiloucas, and B. M. Towlson, "An interferometric technique for measuring terahertz antenna phase patterns", Proc. of the 24<sup>th</sup> Int. Conf. on Infrared and Millimeter Waves, Monterrey (1999).
- [12] S. Hadjiloucas, H.-W. Hübers, J. W. Bowen, and J. Schubert, "Quasi-optical measurements of corner cube antenna amplitude and phase patterns at 1397.1 GHz", IOP Proc. of the Appl. Optics and Opto-Electronics Conf., 77 (2000).